PHYSICAL REVIEW B **68**, 041307(R) (2003)

Spatial imaging of magnetically patterned nuclear spins in GaAs

J. Stephens, R. K. Kawakami, J. Berezovsky, M. Hanson, D. P. Shepherd, A. C. Gossard, and D. D. Awschalom
Center for Spintronics and Quantum Computation, University of California, Santa Barbara, California 93106, USA
(Received 26 January 2003; revised manuscript received 17 March 2003; published 25 July 2003)

We exploit ferromagnetic imprinting to create complex laterally defined regions of nuclear spin polarization in lithographically patterned MnAs/GaAs epilayers grown by molecular beam epitaxy. A time-resolved Kerr rotation microscope with $\sim 1\ \mu$m spatial resolution uses electron spin precession to directly image the GaAs nuclear polarization. These measurements indicate that the polarization varies from a maximum under magnetic mesas to zero several microns from the mesa perimeter, resulting in large ($\sim 10^4$ T/m) effective field gradients. The results reveal a flexible scheme for lateral engineering of spin-dependent energy landscapes in the solid state.

DOI: 10.1103/PhysRevB.68.041307 PACS number(s): 73.61.Ey, 76.70.Fz, 78.47.+p, 75.70.−i

The ability to control nuclear and electron spin in solids is attracting increased interest for use in spintronics and quantum computation.[1,2] One possible route toward achieving such control is the recently discovered ferromagnetic imprinting of nuclear spins.[3] In this process, a ferromagnetic film induces large (up to ~20%) nuclear spin polarization in an adjacent GaAs epilayer under photoexcitation. This nuclear polarization in turn generates strong effective magnetic fields (up to ~0.9 T) that act on free-carrier electron spins through the contact hyperfine interaction. While ferromagnetic imprinting was previously studied in continuous films, the ability to imprint a complex, spatially varying magnetization onto the semiconductor nuclear spins via lithographic patterning of the adjacent ferromagnet may offer a route towards novel spin-based devices. In this case, laterally defined nuclear domains should result in spatially varying effective magnetic fields and field gradients, giving rise to local enhancement of the electron Larmor precession frequency and spin-dependent forces on electrons, respectively.

In this paper we investigate how closely the nuclear polarization in the GaAs tracks the magnetization of patterned ferromagnet structures using a low-temperature time-resolved Kerr microscope (TRKM) with $\sim 1\ \mu$m resolution. We find that the spatial variation of the GaAs nuclear polarization approximates the shape of the patterned ferromagnet, with a transition from maximum to zero nuclear polarization occurring over a distance Λ of $\sim 10\ \mu$m, yielding effective magnetic field gradients of $\sim 10^4$ T/m at $T = 5$ K. We also find that Λ remains roughly constant with increasing temperature, in contrast to the electronic mobility. This suggests that the longitudinal electron spin lifetime may play a role in setting the transition width. Finally, we observe a monotonic decrease in Λ with increasing GaAs epilayer thickness as well as fluctuations in the nuclear polarization as a function of lateral position under the ferromagnet.

Samples are grown by molecular beam epitaxy (MBE) and have the following structure: type-A MnAs(15 or 25 nm)/*n*-GaAs(100, 250, 500 nm)/$Al_{0.75}Ga_{0.25}As$(400 nm)/n^+-GaAs(100) substrate. The *n*-GaAs layer was Si doped at nominally 7×10^{16} cm^{-3}. Figure 1(a) shows an optical micrograph of an array of 100 μm$\times$100 μm square MnAs mesas defined by optical lithography followed by a chemically selective wet etch (1 min HCl:H_2O, 1:10). Comparison of hysteresis loops for a patterned and an unpatterned sample taken at $T = 5$ K in a commercial superconducting quantum interference device magnetometer (SQUID) [Fig. 1(b)] reflect unchanged bulk magnetic properties. Magnetic force microscopy (MFM) of a magnetized MnAs mesa indicates that a single magnetic domain extends to the mesa edges in zero applied field as shown in Fig. 1(c), while atomic force microscopy (AFM) (not shown) identifies mesa sidewall widths of ~100 nm, lateral edge roughness of $<1\ \mu$m, and MnAs root-mean-square (rms) vertical roughness of ~0.4 nm. Samples are mounted face down onto *c*-axis sapphire using a transparent epoxy and the substrate is removed up to the 400-nm AlGaAs layer using a chemically selective etch.

Nuclear polarization in the GaAs layer is determined by measuring the Larmor precession frequency of electron spins via time-resolved Kerr rotation.[4,5] The measurement is performed with the TRKM (Ref. 6) [Fig. 2(a)] which is used to image electron spin dynamics in GaAs with $\sim 1\ \mu$m resolution from $T = 5$ K to room temperature. Pump and probe pulses from a Ti:sapphire laser (~150 fs pulse width, 76 MHz repetition rate, wavelength ~815 nm) are focused through a microscope objective (numerical aperture = 0.73)

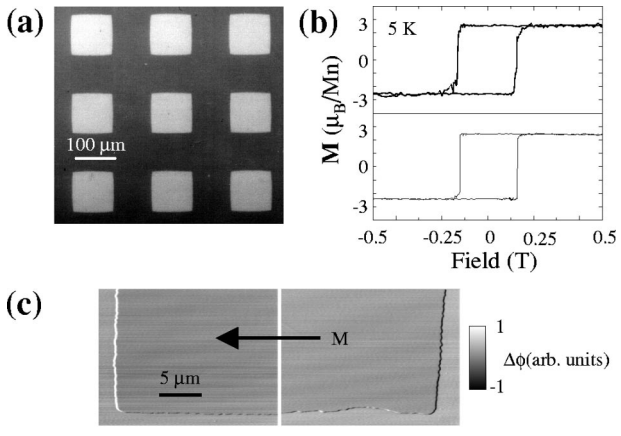

FIG. 1. (a) Optical micrograph of MnAs mesas. (b) Hysteresis loops taken at 5 K with field//GaAs[110] in a commercial SQUID for patterned (top) and unpatterned (bottom) MnAs epilayers. (c) Two different MFM images showing phase ($\Delta\phi$) contrast between the left and right edges of the same MnAs mesa indicating a single magnetic domain magnetized in plane.

 ©2003 The American Physical Society

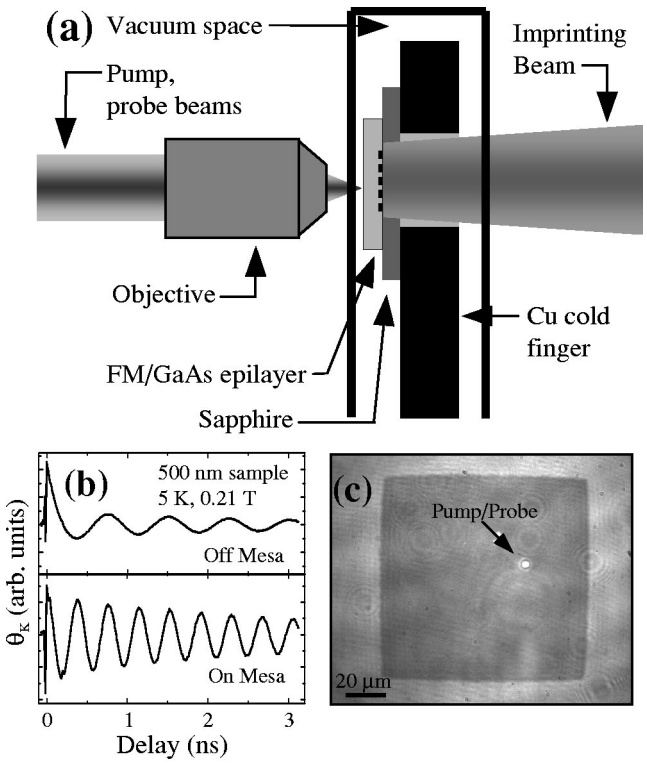

FIG. 2. (a) Schematic of the experimental geometry. (b) Larmor precession of electron spins underneath a MnAs mesa (bottom) and between mesas (top). (c) CCD image of a MnAs mesa taken through the microscope objective showing the small overlapped pump and probe spots.

which can be scanned laterally with ~20 nm precision. The circularly polarized pump pulse (~450 μW) incident normal to the sample excites spin-polarized electrons in the GaAs layer in the direction of its propagation. After a time delay Δt, a linearly polarized probe pulse (~350 μW) passes through this nonequilibrium spin population and experiences a Kerr rotation θ_K proportional to the component of net spin normal to the GaAs layer. The temporal evolution of this net spin polarization is obtained by measuring θ_K while scanning Δt. In the presence of a transverse magnetic field, the electron spins precess coherently in a plane perpendicular to the field at the Larmor frequency ν_L. Here ν_L is proportional to the total effective transverse field comprised of the applied field (B_{app}, set to 0.21 T) and the nuclear contact hyperfine field (B_N) and is given by $\nu_L = g\mu_B(B_{\mathrm{app}}+B_N)/h$, where μ_B is the Bohr magneton and $g=-0.44$ for GaAs. In general, the Larmor frequency may be modulated by other effects (e.g., fringing fields); however, as discussed below, they contribute negligibly to ν_L in these experiments. In our experiment the Larmor precession manifests as an exponentially damped cosine $\theta_K(\Delta t) = A\exp(-\Delta t/T_2^*)\cos(2\pi\nu_L\Delta t)$, where T_2^* is the effective transverse spin lifetime. Thus fitting θ_K as a function of Δt yields a measure of B_N, which in turn is proportional to the nuclear polarization.[7–9] In addition to the pump and probe beams, a third linearly polarized beam (813 nm, 30 mW continuous-wave diode laser) is incident to the sample through the sapphire and serves to excite the photocarriers in the GaAs necessary to establish the nuclear imprint.[3,10] This "imprinting" beam is defocused to a spot size of ~500 μm to provide broad, slowly varying illumination over the scan area. Figure 2(b) shows a delay scan taken at the center of a MnAs mesa as well as one taken on the bare GaAs between two mesas. The higher precession frequency on the mesa indicates the presence of nonzero nuclear polarization corresponding to B_N of ~0.2 T.

Figure 2(c) shows a charge-coupled-device (CCD) image of the tightly focused pump and probe beams as well as the centermost region of the large imprinting beam (which provides the background illumination) on a MnAs mesa. To ensure that the pump and probe beams do not significantly alter the nuclear polarization created by the imprinting beam, we study the nuclear polarization as a function of laboratory time after turning on the pump and probe. We observe an increase in ν_L of $<5\%$, indicating that the effect of the pump-probe beams is negligible compared to the imprinting beam. In addition, we note that because the imprinting beam is linearly polarized, nuclear polarization induced by optically driven dynamic nuclear polarization is negligible.[9,11]

In order to quantify how precisely the nuclear polarization tracks the shape of the MnAs mesas, we construct two-dimensional images of B_N by scanning the microscope objective relative to the fixed sample and performing a time delay scan at each position. Figures 3(a) and 3(b) depict 150 μm$\times$150 μm scans (3 μm step size) of B_N over a MnAs mesa for samples of GaAs epilayer thickness of 100 and 500 nm, respectively. Qualitatively, these plots show a transition from maximum nuclear polarization under the MnAs mesas to zero nuclear polarization in regions where the MnAs has been etched away. Analysis of individual line scans over the mesa edge [Fig. 3(c)] yields the transition width Λ, which we define as the distance over which B_N increases from 10% to 90% of its average value under the mesa, $\langle B_N\rangle$. Comparing the two samples, Λ is larger for the sample with 500 nm of *n*-GaAs. Furthermore, for the 100-nm sample the average effective field $\langle B_N\rangle$ is 0.34 T (6% polarization) and the maximum gradient is 4.4×10^4 T/m, while these values are 0.28 T (5% polarization) and 1.8×10^4 T/m for the 500-nm sample.

Another striking feature of the data is the appearance of fluctuations in the magnitude of nuclear polarization as a function of lateral position on the sample, which do not correlate to any morphological features measured via AFM. These fluctuations in the nuclear polarization are more evident in the 100-nm sample [Fig. 3(a), left panel] than in the 500-nm sample. To determine whether they are associated with inhomogeneity in the imprinting beam or are associated with sample inhomogeneity, the imprinting beam is translated laterally and the nuclear polarization is imaged a second time. We find that the structure in the nuclear polarization is independent of imprinting beam position, indicating that the fluctuations are due to some sample inhomogeneity. Additional measurements performed on unpatterned samples show similar behavior, indicating that the fluctuations are not an artifact of the MnAs lithography and that the decrease in nuclear polarization at the edge of a mesa is not due to spatial variation of the imprinting beam intensity. Finally, Fig.

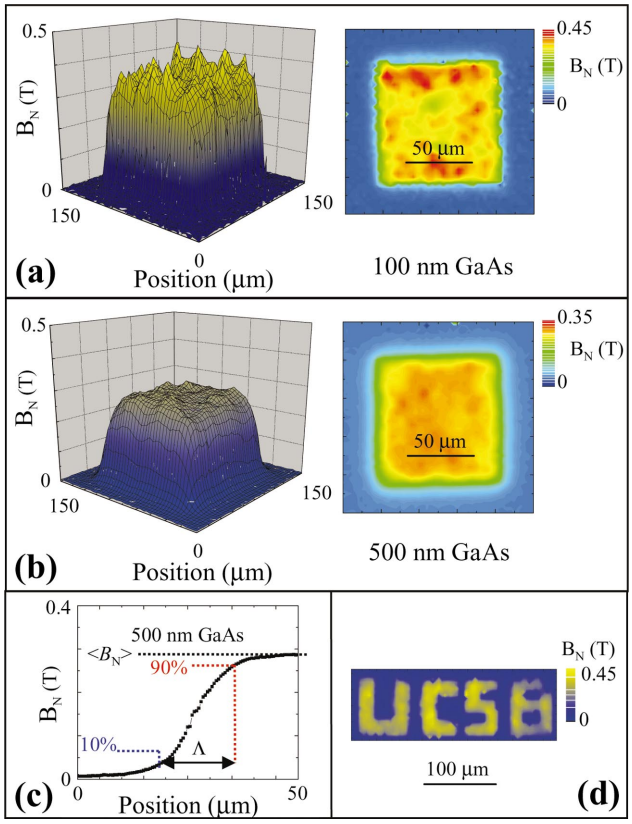

FIG. 3. (Color) (a), (b) Spatial images of ferromagnetically imprinted nuclear domains in 100 and 500-nm-thick *n*-GaAs epilayers, respectively, measured at 5 K and 0.21 T applied field. The scale in the surface plots is the same in each case, while in the color map plots it is optimized for each sample. (c) A line scan on the 500-nm GaAs sample (0.5 μm step size) illustrating the definition of Λ. (d) Spatial image showing a more complex nuclear domain pattern.

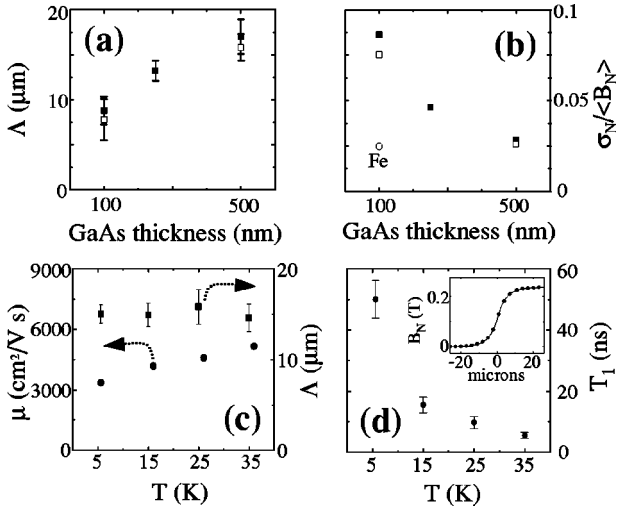

FIG. 4. (a) Nuclear polarization transition width Λ as a function of GaAs thickness for two sample sets grown on different substrates. (b) Fluctuation in nuclear polarization $\sigma_N/\langle B_N\rangle$ as a function of epilayer thickness for two sample sets, where σ_N is the standard deviation and $\langle B_N\rangle$ is the mean of B_N under a MnAs mesa. Also shown (open circle) is one measurement on a sample with Fe in place of MnAs. (c) Transition width (squares) and electronic mobility (circles) as a function of temperature on the 500-nm sample. (d) Fitted values of T_1 based on measured linecuts of nuclear polarization as a function of temperature. Inset: measured linecut of nuclear polarization (solid circles) and fit (solid line) of nuclear polarization that yields T_1 at $T=5$ K for the 500-nm-thick *n*-GaAs epilayer.

3(d) demonstrates that spreading of the nuclear polarization does not preclude the ability to define more complex nuclear domains.

The value of the width over which the nuclear polarization decreases, averaged over the mesa edges [Fig. 4(a), solid squares], yields values of $\Lambda=9$, 13, and 17 μm for GaAs thicknesses of 100, 250, and 500 nm, respectively, at 5 K. As a measure of the fluctuations in B_N, we calculate the standard deviation (σ_N) divided by the mean ($\langle B_N\rangle$) for the center 60 μm$\times$60 μm region of the 100 μm$\times$100 μm mesas. These data [Fig. 4(b), solid squares] show that the magnitude of the fluctuations decreases markedly with increasing GaAs thickness. We verify these trends in Λ and $\sigma_N/\langle B_N\rangle$ as a function of GaAs thickness by fabricating a second sample set (with identical GaAs thicknesses) from a new set of wafers. The results for Λ and $\sigma_N/\langle B_N\rangle$ are summarized by the open squares in Figs. 4(a) and 4(b), respectively. The agreement between the two sample sets indicates that these quantities are robust even in the presence of growth-to-growth variations in the base material.[12] We also note that this consistency in Λ and $\sigma_N/\langle B_N\rangle$ remains despite the presence of sample-to-sample variation in the magnitude of B_N.

To investigate the origin of the fluctuations in nuclear polarization, we measure the nuclear polarization for a 100 nm GaAs layer covered by 12 nm of MBE-deposited Fe [open circle in Fig. 4(b)].[13] We observe that $\sigma_N/\langle B_N\rangle$ for the Fe sample is significantly lower than that of a MnAs sample with equal GaAs thickness. This seems to indicate that the fluctuations are not driven by processes in the GaAs layer, but rather stem from variation inherent to the ferromagnet or ferromagnet/GaAs interface. We note that the lattice mismatch of the MnAs/GaAs system is larger than that of Fe/GaAs and that the nucleation processes during the growth of these two materials differ significantly.[14–16] These differences may result in spatial variation in the efficiency of the ferromagnetic proximity polarization (FPP) of electron spin, which is known to be an underlying mechanism driving the nuclear polarization.[10] In addition, scans of MnAs samples at $T=60$ K (at which there is negligible nuclear polarization) show spatially uniform ν_L, indicating that the nuclear polarization fluctuations observed at $T=5$ K are not due to inhomogeneous strain-induced changes in the Landé g factor. These high-temperature measurements also place an upper bound on contributions to ν_L from sources other than the applied and nuclear fields. For instance, one may reasonably expect that fringing fields (since the Curie temperature[16] of MnAs is 313 K) or Rashba splitting (resulting from drift due to strain-induced inhomogeneous band bending) would result in some modification of ν_L near the mesa edges. While these effects may indeed be present, they are not large enough to detect.

Finally, we investigate whether the electronic mobility is involved in determining Λ. Since photoexcited electrons polarized via the FPP process are necessary to generate the nuclear polarization, the magnitude of Λ is likely related to the motion of these carriers (via drift or diffusion). Because the diffusion length and drift velocity both depend on electron mobility μ ($\ell_{\mathrm{diff}} \sim \sqrt{\mu}, \nu_{\mathrm{drift}} \sim \mu$), we investigate the role of electron motion by comparing the temperature dependence of μ and Λ for one of the 500-nm samples. Measurements from $T=5$ to 35 K [Fig. 4(c), solid squares] show that Λ remains approximately constant as a function of temperature.[17] Mobility measurements are performed on Hall bars[18] at similar temperatures and under approximately the same illumination intensity as that provided by the imprinting beam [Fig. 4(c), solid circles]. We find that μ increases with temperature, from a value of 3400 $\mathrm{cm}^2/\mathrm{V\,s}$ at $T=5$ K to 5100 $\mathrm{cm}^2/\mathrm{V\,s}$ at $T=35$ K. This discrepancy in the temperature dependences of Λ and μ indicates that a simple model explaining Λ in terms of only the electron drift and diffusion is inadequate. Other factors such as the electron spin lifetime, enhanced electron spin diffusion,[19,20] and interfacial reflection of electrons[21] must be considered. In particular, one explanation for the different temperature dependences of Λ and mobility may be related to a decrease of the longitudinal electron spin lifetime T_1 with increasing temperature.[22] Given the temperature dependence of the mobility, we calculate an approximate T_1 by fitting linecuts of nuclear polarization with a simple model that estimates the steady-state diffusion profile of electron spin emanating from beneath the MnAs mesas.[23] Figure 4(d) shows an order of magnitude decrease (50–5 ns) in T_1 as calculated from the model from $T=5$ to 35 K, as well as a representative linecut and fit of B_N (inset). Another potential factor in determining Λ is the diffusion of nuclear spin, but to date we have not observed propagation of nuclear domain boundaries with time scales characteristic of nuclear diffusion ($\sim$minutes).[24]

In conclusion, we have demonstrated the patterning and imaging of nuclear spin domains whose hyperfine fields may be exploited for manipulating electron spin in novel spintronic devices.

The authors wish to thank R. J. Epstein and D. K. Young for technical assistance and E. Johnston-Halperin and Y. Kato for stimulating discussions. We acknowledge support from Grant Nos. DARPA/ONR N00014-99-1-1096, AFOSR F49620-02-10036, ARO DAAD 19-01-1-0541, and NSF DMR-0071888.

[1] D. Loss and D. P. DiVincenzo, Phys. Rev. A **57**, 120 (1998).
[2] B. E. Kane *et al.*, Nature (London) **393**, 133 (1998).
[3] R. K. Kawakami *et al.*, Science **294**, 131 (2001).
[4] J. M. Kikkawa *et al.*, Science **277**, 1284 (1997).
[5] S. A. Crooker *et al.*, Phys. Rev. Lett. **77**, 2814 (1996).
[6] W. K. Hiebert, A. Stankiewicz, and M. R. Freeman, Phys. Rev. Lett. **79**, 1134 (1997).
[7] D. Paget, G. Lampel, and B. Sapoval, Phys. Rev. B **15**, 5780 (1977).
[8] J. M. Kikkawa and D. D. Awschalom, Science **287**, 473 (2000).
[9] G. Salis *et al.*, Phys. Rev. Lett. **86**, 2677 (2001).
[10] R. J. Epstein *et al.*, Phys. Rev. B **65**, 121202(R) (2002).
[11] Optically induced DNP is not strictly zero due to the presence of an applied field. The level of nuclear polarization due to this process with our modest field ($\sim$0.2 T), however, is negligible, as shown in Ref. 9.
[12] Of the two 500-nm samples shown in Figs. 3 and 4, one had 15 nm of MnAs while the other had 25 nm.
[13] Fe grown at room temperature, growth rate $\sim$0.1 nm/min.
[14] G. A. Prinz and J. J. Krebs, Appl. Phys. Lett. **39**, 397 (1981).
[15] M. Tanaka, Semicond. Sci. Technol. **17**, 327 (2002).
[16] F. Schippan *et al.*, Appl. Phys. Lett. **76**, 834 (2000).
[17] We note that although there is some mesa-to-mesa and sample-to-sample variation in the temperature dependence of Λ, all measurements have shown flat or slightly decreasing Λ with temperature.
[18] Hall bars with indium contacts were patterned from the *n*-GaAs epilayer after removal of MnAs and were driven with 1 μA current. Under illumination, a carrier density of $n=6\times10^{15}\ \mathrm{cm}^{-3}$ was obtained.
[19] J. M. Kikkawa and D. D. Awschalom, Phys. Rev. Lett. **80**, 4313 (1998).
[20] M. E. Flatté and J. M. Byers, Phys. Rev. Lett. **84**, 4220 (2000).
[21] L. Sham *et al.*, Phys. Rev. Lett. **89**, 156601 (2002).
[22] P. H. Song and K. W. Kim, Phys. Rev. B **66**, 035207 (2002).
[23] Our model assumes that the MnAs mesa acts as a step function source $S(x)$ of electron spin, which results in a spin distribution $F(x,t)$ given by $\partial F/\partial t = D_e \partial^2 F/\partial x^2 - F/T_1 + S(x)$. By modeling our data with the steady-state spin distribution we obtain a value for the product $D_e T_1$ where D_e is the electron diffusivity. We can thus calculate "T_1" using the Einstein relation between mobility and diffusivity.
[24] D. Paget, Phys. Rev. B **25**, 4444 (1982).